

# Design of a Six-Port Reflectometer for a Microwave Breast Cancer Detection System

Marek E. Bialkowski, Norhudah Seman and Wee Chang Khor

*School of Information Technology and Electrical Engineering, The University of Queensland,  
St. Lucia, Queensland 4072, Australia*

*Email: meb@itee.uq.edu.au, norhudah@itee.uq.edu.au and khor@itee.uq.edu.au*

## Abstract

*The design of a wideband microwave reflectometer for the purpose of inclusion in a breast cancer detection system is presented. In this system, a wideband frequency source is used to synthesize a narrow pulse via the step-frequency synthesis method. The reflectometer undertakes measurements in frequency domain and the collected data is transformed into time/space domain using IFFT. In order to accomplish reflection coefficient measurements over a large frequency band, wideband couplers, dividers and square-law power detectors are required to form the six-port reflectometer. In this measurement equipment, voltages appearing at the detectors outputs can be processed with a PC equipped with precision Analogue to Digital converters. The chosen configuration of the six-port enables the display of the measured data in real-time. Its operation is studied with the use of Agilent ADS.*

## 1. Introduction

Breast cancer is the most common cancer diagnosed in women in various parts of the world. In Australia alone, it is estimated that one in eleven Australian women will develop breast cancer at some stage in their life [1].

Early detection and effective treatment is the only way to reduce the mortality rate due to breast cancer. Currently the primary method for breast screening is X-ray mammography [2], [3].

X-ray mammography has saved many lives, but the technology still produces a relatively high number of false negative and false positive diagnoses. There is also health concern related to exposure to ionizing radiation [3]. These factors have generated interest in alternative approaches of breast cancer detection that feature various degree of success. For example ultrasound is used clinically to discover whether a lesion detected in a mammogram is a liquid cyst or a solid tumour [2]. In addition, Magnetic Resonance Imaging has been shown to be a very useful screening tool, but is very expensive and not portable [4].

Recently, microwave imaging has been proposed as a viable alternative to X-ray mammography. Microwave imaging system is essentially "breast tissue radar". It involves an application of very low levels (1000 times less than a mobile phone) of microwave energy through the breast tissue. The foundation for tumour detection is a difference between the electrical properties of normal and malignant breast tissue. Normal breast tissue is largely transparent to microwave radiation while lesions, which contain more water and blood, scatter microwaves back towards the microwave source. The antenna picks up these reflected signals and they are analysed using a computer. A three dimensional image showing the location of the cancerous tissue can be obtained as the outcome of this signal processing [3].

Several research groups, including the University of Wisconsin-Madison and Dartmouth College of the US, University of Calgary in Canada, Technical University Denmark and others are currently doing research in this new area [2], [3], [5]. Similar activities have also been undertaken in the School of ITEE at the University of Queensland in Australia.

The majority of the developed microwave breast cancer detection prototypes are based on the synthesized pulse technique, in which a narrow pulse is generated in the frequency domain [6]. This synthesized signal is launched and received by an antenna which can be moved in small steps across a planar or curved area in front of an imaged object. At each location of the probe antenna, the received signal is processed with a Vector Network Analyser (VNA) which, by using its time domain capability, provides a suitable signal transformation from frequency to time or space domain. The measurement system is controlled from a PC. The collected data is gathered and processed by the PC to obtain a visual insight.

The use of the conventional VNA with time-domain processing capability is handy to test and proof the concept of the microwave breast cancer detection system. Standard microwave laboratories are usually equipped with VNAs to perform various types of microwave

measurements. However, due to their large size and high cost they may be precluded in a commercial breast cancer detection system.

The purpose of the work presented in this paper is to replace the conventional VNA by a low-cost alternative in the form of a wideband microwave six-port reflectometer. This paper is organised as follows, Section 2, describes the experimental setup required for a microwave breast cancer detection system and provides results obtained using the conventional VNA with time-domain processing capability. Section 3 describes the design of a wideband reflectometer. Section 4 shows the results of Agilent ADS simulations of the chosen configuration of the six-port. Finally, Section 5 concludes the paper.

## 2. Experimental System

The configuration of the prototype Microwave Imaging System for breast tumour detection is shown in the Figure 1. The system consists of a mechanical scanning platform in the X-Y direction. The scanning platform supports a wideband probe antenna with the transition to a coaxial line, which in turn is connected to a microwave Vector Network Analyser. The VNA is capable of measuring the full set of S-parameters of a 2 port system (for example when two antennas are used in the detection system). However, in typical prototypes, only the reflection coefficient is required to be measured. Prior to measurements, the system has to be calibrated. For the reflectometer mode of operation, broadband coaxial standards: short, open and match can be used to calibrate the system at the coaxial port at which the probe antenna is connected.

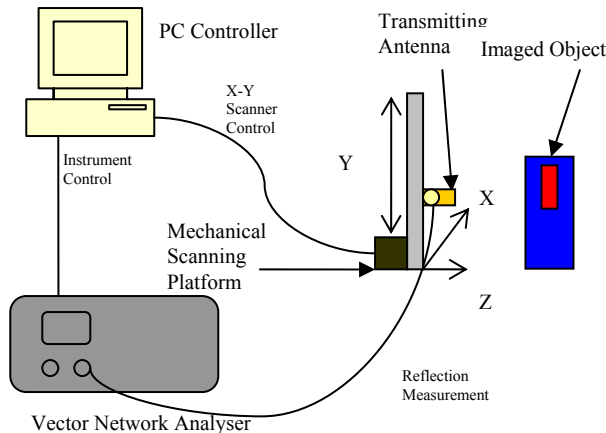


**Figure 1.** The configuration of the microwave imaging system

The prototype system at the University of Queensland is controlled by a PC controller and the measurement procedure includes the following steps:

- 1) Specification of the area to be scanned in the X-Y plane including steps in the X and Y directions.
- 2) At each specified X-Y location, the PC controller triggers the source in the Vector Network Analyser and 50 to 800 (depending on specifications) measurement points over the frequency band of interest are taken. Then, they are converted to the time/space domain.
- 3) Having obtained the frequency and time domain data for a given location, the results are stored in the PC and the probe is moved to a new position and the measurement procedure is repeated.

The obtained data is assembled to create an image. Using false colour scheme, the location of a cancerous tissue can be shown in a colour that is distinctive from the one representing the healthy tissue.

The imaging capabilities of the above-described Microwave Imaging System were tested with respect to a simple breast phantom. This phantom consists of a circular cylindrical plastic container with a diameter of 12.5cm with thickness of 1mm, which can be filled with air or liquid dielectric. A solid material representing a target tumour can be located inside the container. Other solid dielectric materials like rubber can be put around the container to emulate, for example, a lossy breast skin layer.

Figure 2 shows the measured result in which the container is filled with air and a highly reflective object, a copper pipe of diameter 1.2cm and length of 2.1 cm located close to the centre of the plastic container.

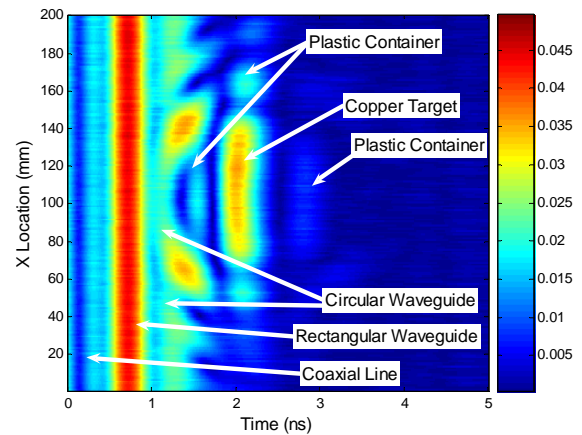


**Figure 2.** The Time domain Reflection Measurement result for Plastic container filled with air and using the standard calibration procedure

In measurements, scanning over a length of 20cm with a resolution of 1mm along the X axis was performed. Reflection coefficient measurements were taken for the vertical polarisation of the probe antenna over the frequency range from 8.2 to 12.4GHz.

The results shown in Figure 2 clearly reveal the location of the copper target and parts of the plastic container. However, a lot of unwanted reflections due to impedance mismatch between the coaxial line and rectangular waveguide, the rectangular wave guide to circular waveguide transition and the circular waveguide to air interface are also observed. They obscure the detection process of the target.

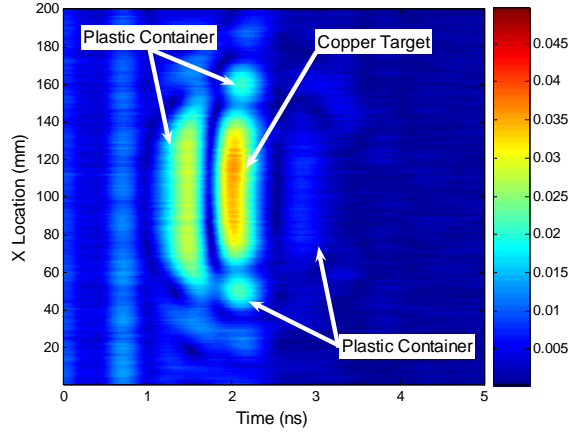


**Figure 3.** The Time domain Reflection Measurement result for Plastic container filled with air and using the modified calibration technique

To improve the detection capability of this Microwave Imaging system, the VNA was calibrated using a special procedure. The coaxial short and shielded standards were used as in the conventional calibration procedure, as followed from the VNA calibration menu. However the coaxial match termination was replaced by a load realized by the probe antenna radiating a microwave signal in free space. The results concerning this modified calibration procedure are shown in Figure 3. As observed in Figure 3, the undesired reflections inside the probe antenna and at the antenna-air interface are considerably reduced. However, the border of the plastic container (circular in shape) and the location of the copper pipe remain identifiable.

### 3. Six Port Design

Our next goal is to replace the VNA (of Figure 1) by a six-port reflectometer composed of wideband couplers, dividers and scalar detectors. The configuration of the six-port which is investigated here is shown in Figure 4. This configuration, introduced in [7], offers real-time display of the measured complex reflection coefficient [8-10].

The chosen configuration of the six-port reflectometer includes quadrature hybrids (Q), and two-way power dividers (D). Also shown in Figure 4 are scalar power detectors connected to ports 3-7, a microwave source

connected to port 1 and a Device Under Test (DUT) connected to port 2. The part of the reflectometer enclosed by a broken line is called a Complex Ratio Measuring Unit (CRMU) or correlator. The Q hybrid outside the CRMU is employed to redirect signals  $a, b$  to perform reflection-type measurements. Other configurations outside the CRMU can be used to re-direct signals  $a, b$  to perform transmission-type measurements. The divider D, outside the CRMU, terminated in a detector is used to monitor the signal source power level. It can be used in a feedback loop to maintain a constant power level from the source. Assuming that all of the power detectors are identical and operate in the square-law power region (meaning that the output current or voltage is proportional to the incident power on the detector), it can be shown using the circuit theory that the reflection coefficient,  $\Gamma$  of the Device Under Test (DUT) is related to the measured power values  $P_3, P_4, P_5, P_6, P_7$  (being proportional to the voltages at the detectors outputs) by the following expression (1) [7] [9].

$$\Gamma = \frac{a}{b} = \Gamma_1 + j\Gamma_2 = \frac{P_6 - P_7}{P_3} + j \frac{P_4 - P_5}{P_3} \quad (1)$$

This expression indicates that for the reflectometer configuration of Figure 4, the complex reflection coefficient,  $\Gamma$  can be displayed in real-time by measuring voltages at the output of the square-law detectors. In the system controlled via PC, this can be accomplished using a precision ADC card connected to the detectors. The PC monitor can be used to show  $\Gamma$  in the polar or other forms of display.

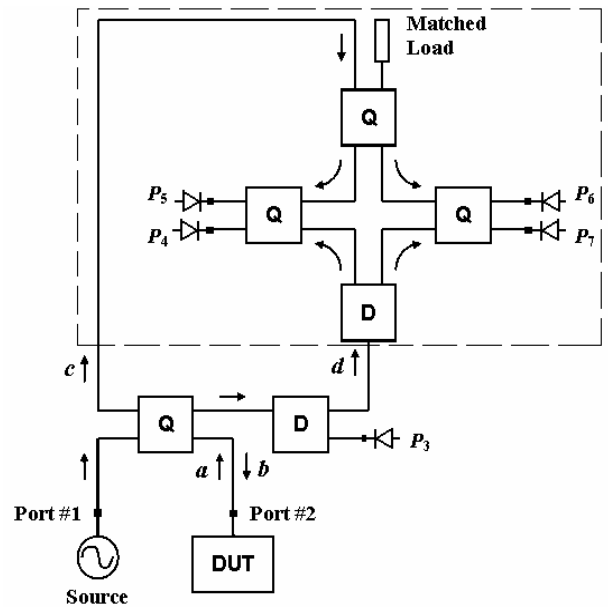


**Figure 4.** Configuration of a six-port reflectometer with the real-time display capability

The six-port reflectometer of Figure 4 can be realized in microstrip or stripline technology. Its wideband performance will depend on the quality of wideband Q and D components, which will be used in its design. At the present stage of our work, we decided to use a Lange coupler [11] as quadrature hybrid (Q) and a Gysel power splitter [12] as a two-way power divider (D) to realize a six-port reflectometer with real-time display capability at least over one octave band.

By assuming the design frequency band from 4 to 8GHz, the performance of individual components was optimized in this band by initially starting the design at the centre frequency of 6GHz. The 3dB designed Lange coupler consists of 8 parallel strips with varying width, spacing and length. The configurations of the chosen Lange and Gysel hybrids are shown in Figure 5.

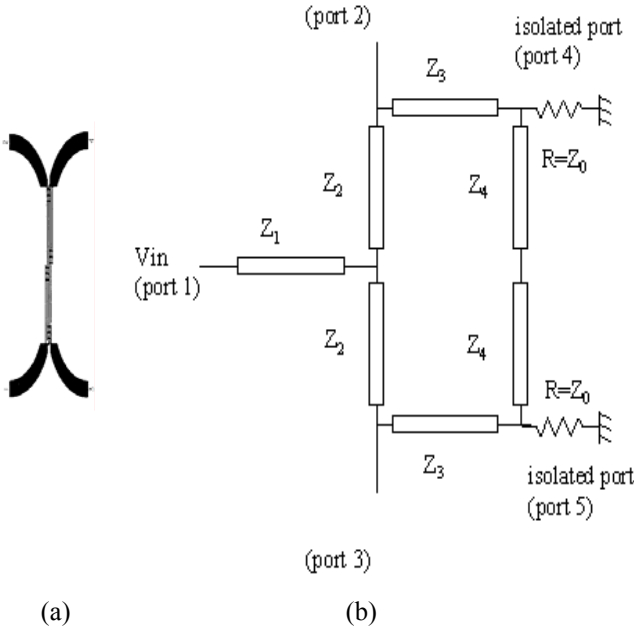


**Figure 5.** Configurations of (a) Lange and (b) Gysel hybrids

#### 4. Simulation Results

The design of individual components forming the six-port reflectometer was performed using Agilent ADS [13]. Following this, the performance of the Complex Ratio Measuring Unit was assessed. Assuming an ideal operation of components forming CMRU and by carrying out derivations similar to those leading to expression (1), it can be shown that the ratio of signals  $c$  and  $d$  entering the CRMU is given by

$$T = T_1 + jT_2 = \frac{c}{d} = \frac{[(P_6 - P_7) + j(P_4 - P_5)]}{d^2} \quad (2)$$

Expression (2) shows that when the source of unit power ( $d^2 = 1$ ) is connected to the input of the CRMU power divider D, the complex ratio,  $T$  can be measured

from differences between the pairs of powers  $P_4$ ,  $P_5$  and  $P_6$ ,  $P_7$ . These, in turn, are related to the squared magnitudes of transmission coefficients  $S_{41}$ ,  $S_{51}$ ,  $S_{61}$ ,  $S_{71}$  assuming that the input port of the CRMU divider D is numbered as 1. To assess the performance of CRMU formed by Lange and Gysel hybrids, in the first instance, a source ( $d=1$ ) was connected at the input of power divider (D) and the quadrature hybrid Q at the top part of CMRU in Figure 4 was match (50 ohm) terminated ( $c=0$ ). The simulation results shown in Figure 6 reveal that for this case the magnitude of  $T$  given by expression (2) is lower than 0.08 within the 4 to 8GHz operating frequency band. In an ideal case the result for  $T$  should be zero. Figure 7 shows the simulated S-parameters of CRMU, which explain the deviation from the ideal case.

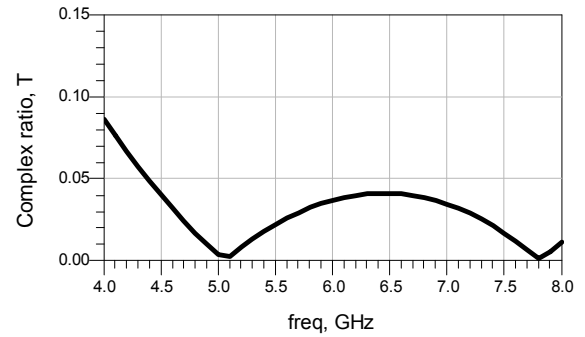


**Figure 6.** Complex ratio  $T=c/d$ , as measured by CMRU when an input port of divider D is fed and top hybrid Q is match terminated

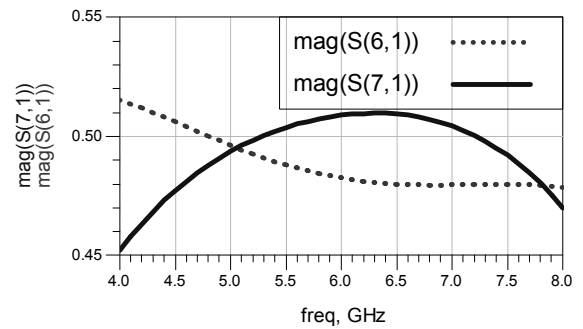
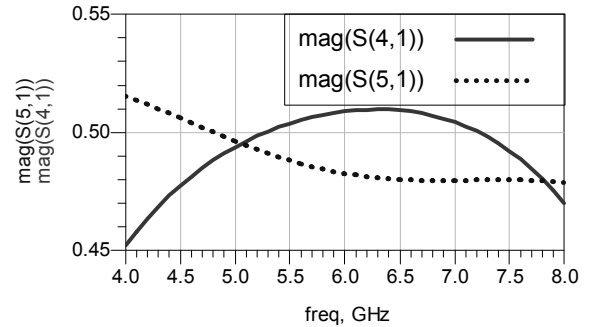


**Figure 7.** CMRU S-parameters for the case when port 1 is an input port of divider D forming CMRU

For  $T$  to be zero magnitudes of  $S_{41}$ ,  $S_{51}$ ,  $S_{61}$  and  $S_{71}$  would need to be equal to 0.5. Figure 7 shows the deviation from this condition.

An alternative test for CRMU concerns the situation in which the divider  $D$  of CRMU is match terminated ( $d=0$ ) and the source ( $c=1$ ) is connected to the top hybrid  $Q$  of CRMU. In this case the input to the top  $Q$  hybrid is numbered as 1. The simulation results for the ratio:  $T'=d/c$  and for the individual S-parameters of CRMU are shown in Figure 8 and 9. Values of magnitude of  $T'$  are comparable with those of  $T$  in Figure 6. The S-parameters of CMRU in Figure 9 provide an explanation why the CMRU did not operate in an ideal manner.

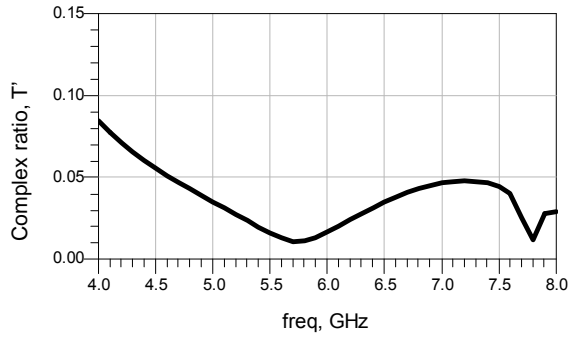


**Figure 8.** Complex ratio  $T'=d/c$  of CMRU when the input port of top  $Q$  hybrid of CRMU is fed and divider  $D$  is match terminated

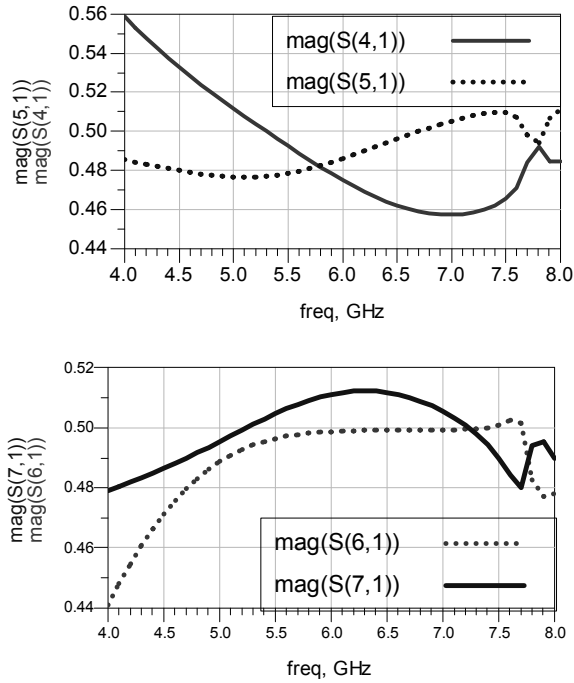


**Figure 9.** CMRU S-parameters when port 1 is formed by the input port of top  $Q$  hybrid of CRMU and divider  $D$  is match terminated

Next simulations concerned the full six-port reflectometer of Figure 4. Figure 10 and 11 show the simulation results of the six port reflectometer of Figure 4 for specific cases of DUT such as short, open and match. Assuming the use of ideal square-law detectors, the reflection coefficient  $\Gamma$  was calculated using expression (3) that is analogous to the one shown in (1):

$$\Gamma = \frac{a}{b} = \Gamma_1 + j\Gamma_2 = \frac{|S_{61}|^2 - |S_{71}|^2}{|S_{31}|^2} + j \frac{|S_{41}|^2 - |S_{51}|^2}{|S_{31}|^2} \quad (3)$$

As observed in Figure 10, the six-port reflectometer gives reflection coefficient  $\Gamma$  of  $0.1 \pm 0.05$  when DUT is in the form of a match load. The deviation from the ideal case is worse than for the CRMU operating alone. This is because coupler  $Q$  and divider  $D$  outside CRMU introduce their own non-ideal performances.

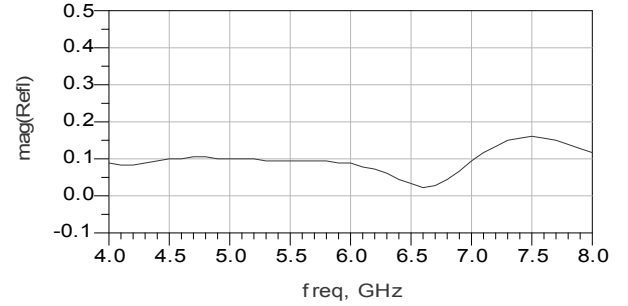


**Figure 10.** Reflection coefficient of the six-port reflectometer with DUT in the form of match load

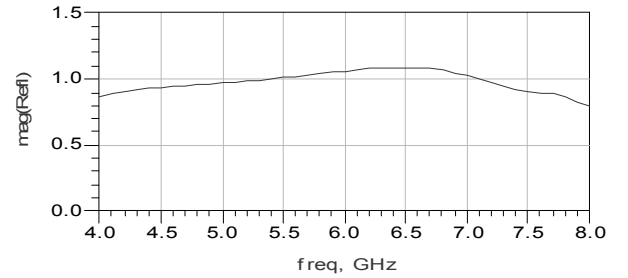
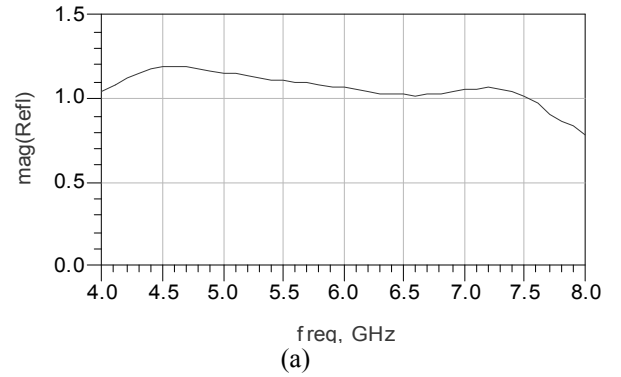


**Figure 11.** Reflection coefficient of the six-port reflectometer with DUT (a) open (b) short

Figure 11(a)-(b) show the simulation results when DUT represents either short or open load. The reflection coefficients,  $\Gamma$  have a magnitude of  $1 \pm 0.2$ . These results indicate a reasonable performance of the real-time display six-port reflectometer over one octave frequency band when Lange coupler and Gysel power dividers are used as building blocks.

The refined performance of the reflectometer can be obtained via a suitable calibration procedure. This is usually accomplished using 5 calibration standards [7] [14]. Obtaining a multi-octave operation will require the use of even more broadband couplers and dividers than the ones investigated here. In this respect, we focus our attention on wideband hybrids, as described in [15-19].

## 5. Conclusion

The design of a wideband microwave reflectometer for the purpose of inclusion in a microwave breast cancer detection system has been presented. In this system, a wideband frequency source is used to synthesize a narrow pulse via the step-frequency synthesis method to illuminate an imaged body. The reflectometer undertakes measurements in frequency domain and the collected data is transformed into time/space domain using an IFFT to locate an object producing a high reflection. A special configuration of a six-port reflectometer which provides the complex reflection coefficient in real-time using simple mathematical transformations of the measured voltages at the outputs of scalar (power) detectors has been described. In order to obtain reflection coefficient measurements over one octave frequency band, wideband Lange couplers and Gysel-type dividers in microstrip technology have been chosen to design such a six-port reflectometer. The operation of this system has been demonstrated via ADS simulations. The work on this system is continued to obtain more precise operation in real-time in a multi-octave frequency band.

## 6. Acknowledgment

The authors acknowledge the financial support of the Australian Research Council via Grants DP0449996 and DP0450118.

## 7. References

[1] Australian Institute of Health and Welfare & Australasian Association of Cancer Registries (AACR), "Cancer in Australia 2001," *AIHW cat. No.CAN23. Canberra: AIHW (Cancer Series no. 28)*, 2004, pp. 64-68.

[2] E.C. Fear, S.C. Hagness, P.M. Meaney, M. Okoniewski and M.A. Stuchly, "Enhancing breast tumor detection with near-field imaging," *IEEE Micro*, March 2002, pp. 48-56.

[3] E.C. Fear P.M. Meaney and M.A. Stuchly, "Microwave for breast cancer detection," *IEEE Potentials*, 2003, pp. 12-18.

[4] MARIBS study group, "Screening with magnetic resonance imaging and mammography of a UK population at high familial risk of breast cancer: A prospective multicentre cohort study," *The Lancet*, vol. 365, 2005, pp. 1769-78.

[5] Title: "Microwave imaging for breast-cancer screening" Available:

[http://www.emi.dtu.dk/research/afg/research/breastcancer\\_screening.html](http://www.emi.dtu.dk/research/afg/research/breastcancer_screening.html)

[6] D.A. Noon and M.E. Bialkowski, "An inexpensive microwave distance measuring system," *Microwave and Optical Technology Letters*, vol. 6, no. 5, April 1993, pp. 287-292.

[7] C.A. Hoer, "A microwave network analyzer using two 6-port reflectometers," *Microwave Symposium Digest, MTT-S International*, vol. 77, issue 1, June 1977, pp. 47-49.

[8] S. Stuchly, M.E. Bialkowski, K. Caputa, and W. Guo, "Microwave level gauging system", *Proc.10th Int. Microwave Conference, MIKON 94*, Ksiaz, Poland, May 30-June 2, 1994, pp. 530-534.

[9] M.E. Bialkowski and A.P. Dimitrios, "A step-frequency six-port network analyser with a real-time display", *AEU Intl. Journal of Electronics and Communications*, vol. 47, no. 3, 1993, pp. 193-197.

[10] G.F. Engen, "An improved circuit for implementing the six-port technique of microwave measurements," *IEEE Trans. Microwave Theory Tech.*, vol. MTT-25, no.12, Dec. 1977, pp. 1080-1083.

[11] J. Lange, "Interdigitated stripline quadrature hybrid", *IEEE Trans. Microwave Theory Techn.*, Dec. 1969, pp. 1150-1151.

[12] U. Gysel, "A new N-way power divider/combiner suitable for high-power applications", *Microwave Symposium Digest, MTT-S International*, vol. 75, no. 1, 1975, pp. 116-118.

[13] Agilent Technologies, *Advanced Design System 2002 - Passive Circuit Design Guide*, Feb. 2002.

[14] M.E. Bialkowski, "Microwave network analyser incorporating a single six-port reflectometer", *AEU Intl. Journal of Electronics and Communications*, vol. 47, no. 3, 1993, pp. 193-197.

[15] J-H Cho, H-Y. Hwang, and S-W. Yun, "A design of wideband 3-dB coupler with N-section microstrip tandem structure", *IEEE Microwave and Wireless Components Letters*, vol. 15, Feb. 2005, pp. 113-115.

[16] M-H Murgulescu, E. Moisan, P. Legaud, E. Penard and I. Zaquine, "New wideband,  $0.67\lambda_g$  circumference 180 hybrid ring coupler", *Electronics Letters*, vol. 30, no. 4, Feb. 1994, pp. 299-300.

[17] J.P. Shelton, J. Wolfe, R.C. Wagoner, "Tandem couplers and phase shifters for multioctave bandwidth", *Microwaves*, April 1965, pp. 14-19.

[18] F.C. de Ronde, "A new class of microstrip directional couplers", *Microwave Symp. Digest*, May 1970, pp. 184-189.

[19] S. Uysal and A.H. Aghvami, "Synthesis and design of wideband symmetrical nonuniform couplers for MIC applications", *IEEE MTT-S Symp. Digest*, 1988, pp. 587-590.